Wave-function collapse with increasing ionization: $4d$ photoabsorption of Cs through Cs^{4+}

A. Cummings, C. McGuinness, and G. O'Sullivan
Department of Experimental Physics, University College Dublin, Dublin 4, Ireland

J. T. Costello, J. P. Mosnier, and E. T. Kennedy
National Centre for Plasma Science and Technology and School of Physical Sciences, Dublin City University, Glasnevin, Dublin 9, Ireland

(Received 21 June 2000; published 5 January 2001)

The $4d$ relative photoabsorption cross section of cesium has been observed to change dramatically in appearance along the isonuclear sequence Cs through Cs^{4+}. In each case, discrete structure is observed below threshold and for Cs through Cs^{2+}, a giant dipole $4d \rightarrow \varepsilon f$ resonance is also present above threshold. Between Cs^{2+} and Cs^{3+}, there is a striking change, with much of the oscillator strength available in the $4d \rightarrow f$ channel being abruptly transferred to the discrete spectrum. Despite the complexity of the transitions involved, the oscillator strength envelope for the discrete transitions yields relatively few features and remains essentially static in energy regardless of the parent terms. Hartree-Fock with configuration interaction and time-dependent local-density-approximation calculations successfully account for this behavior and permit identification of the discrete features.

DOI: 10.1103/PhysRevA.63.022702 PACS number(s): 32.80.Hd, 32.30.Jc, 52.25.Os, 52.50.Jm

I. INTRODUCTION

While the $4d$ absorption spectrum of neutral cesium is known [1], very little information exists on the photoabsorption spectra of cesium ions. In fact, the only work to date has been a study of the valence $5p$ excitation of Xe-like Cs^{+} [2] and a recent observation of discrete features due to $4d \rightarrow nf$ and $4d \rightarrow np$ transitions in the same ion [3]. However, there has been considerable interest, both theoretical and experimental, in changes in the $4d$ photoabsorption spectra with increasing ionization. Such work seems set to acquire new momentum as a result of recent advances in merged beam experiments in which ion beams from electron cyclotron resonance or other sources interact with synchrotron radiation [4–8]. To date, the few experiments performed have largely focused on the Xe isoelectronic sequence where the spectra of Ba^{2+} and La^{3+} have been investigated by the resonance laser driven ionization or dual laser produced plasma (DLP) techniques, respectively [9,10], and the Xe isonuclear sequence, where changes in $4d$ photoabsorption cross section in stages up to and including Xe^{7+} have been studied in merged beam experiments using photoelectron and photoion yield spectroscopy [4,11–13]. In addition, experimental data also exist for changes along the barium and iodine isonuclear sequences in going from the neutral atom to the doubly ionized ion [14,15], while the $4d$ photoabsorption spectra of Sb in stages up to four times ionization have recently been studied [16]. In the present work, we report on the extension of these observations to the Cs isonuclear sequence.

In the neutrals of all these elements, the photoabsorption spectra above the $4d$ threshold are dominated by a broad $4d \rightarrow \varepsilon f$ resonance with some weaker structure due to double electron excitations superimposed, while below threshold discrete transitions that arise from $4d \rightarrow np$ excitation have been identified. Transitions of the type $4d \rightarrow nf$ are absent because of the large centrifugal repulsion present in the $l = 3$ channel that excludes the radial component of the nf wave functions from the core region. In these atoms, the potential has a double well character and the nf wave functions are essentially eigenstates of the outer well [17]. With increasing ionization, the centrifugal barrier disappears and $4f$ wave function contraction into the inner well region results in a transfer of oscillator strength from the continuum to the discrete spectrum [18–22]. We have identified two somewhat different situations whose behavior seems to be determined essentially by whether the $4f$ simply contracts with increasing ionization or collapses abruptly [23]. In practice this may be inferred from the energy positions of the $4d \rightarrow nf$ features in the ion relative to the location, in the neutral atom, of the $4d \rightarrow \varepsilon f$ resonance. It can be attributed to the fact that the shape of the inner well does not change appreciably with the valence ionization. As a result, the center of gravity and overall shape of the $4d \rightarrow \varepsilon f$ oscillator strength distribution was shown to remain essentially static with increasing ionization [24,25].

In Sb, and one suspects in the other elements immediately preceding Xe in the Periodic Table, an increase in ionization is seen to produce a gradual erosion of the $4d \rightarrow \varepsilon f$ resonance with the oscillator strength that is removed being shared among the subthreshold $4d \rightarrow nf$ transitions. This behavior reflects a gradual contraction with no ''sudden'' collapse of the $4f$ orbital. In Sb, for example, the $4d \rightarrow nf$ features, in stages up to Sb^{4+}, do not extend into the region of the peak of the neutral $4d \rightarrow \varepsilon f$. However, at higher Z and certainly along the Xe isoelectronic sequence where the $4d \rightarrow nf$ features are found within the envelope of the neutral $4d \rightarrow \varepsilon f$ resonance, there is an abrupt redistribution of the oscillator strength from the resonance to the discrete spectrum between the second and third ionization stages. The situation for the Xe isonuclear sequence appears to be intermediate between these two extremes and indeed the theoretical evidence favors contraction [20,23]. The results for Xe^{3+} [13], where the oscillator strength seems to be shared between the discrete spectrum and the continuum in almost

equal measure, suggest that in going from Xe^{2+} to Xe^{3+} there is a significant change in the cross section, though not as pronounced as in going from Ba^{2+} to La^{3+}. By Xe^{4+}, the oscillator strength is certainly concentrated in the discrete spectrum [4].

This behavior may be also be understood in terms of the relative positions of the $4d^9 4f_{\mathrm{av}}$ (average energy of configuration) ^1P and $4d^9 4f^1P$. In Xe and the elements immediately preceding it, the $4d \rightarrow \varepsilon f$ resonance is reproduced in a Hartree-Fock calculation from consideration of continuum functions, while the $4f_{\mathrm{av}}$ function is uncollapsed. Past xenon, the $4f_{\mathrm{av}}$ is an inner well function and the resonance may be interpreted as an autoionization of the $4d^9 4f_{\mathrm{av}}{}^1P$ state. Complete collapse occurs when the $4d^9 4f_{\mathrm{av}}{}^1P$ and $4d^9 4f^1P$ are essentially the same. Because of the differing behaviors of $4d^9 4f_{\mathrm{av}}{}^1P$ and $4d^9 4f^1P$, the labeling of the discrete states in all cases is very sensitive to the choice of basis used in any calculations. The lowest $4d^9 nf$ states are strongly LS coupled and their wave functions are highly term dependent [26,27]. The validity of using the configuration average approach, in which the term-dependent wave functions are synthesized from configuration average ones, has been discussed by Wendin and Starace [28]. They have shown that the approaches are equivalent, but some confusion with regard to the labeling of states may arise, though the ''correct'' labels may be inferred from counting the number of nodes in the appropriate wave functions.

In a multiconfiguration Hartree-Fock (MCHF) average energy of configuration (E_{av}) calculation, the $4d^9 nf$ terms are thus very highly mixed and each $4d^9 nf$ level has a small $4d^9 4f_{\mathrm{av}}{}^1P$ component. Once the $4f_{\mathrm{av}}$ radial function has collapsed it becomes localized in the core region and has a large spatial overlap with the $4d$ wave function. As a result, the different $4d^{10} \rightarrow 4d^9 nf$ transitions have appreciable oscillator strength and are generally stronger than the $4d \rightarrow np$ lines. Thus, in the first ion stages of any of the species studied, transitions to nf final states appear with good intensity. As the degree of ionization increases, both the $4f_{\mathrm{av}}$ and $4f$ wave functions collapse, but at different rates, so that the $4f$ better approximates the $4f_{\mathrm{av}}$ as the ion becomes more highly charged. Moreover, the level separation increases so that the nf $(n>4)$, $4f_{\mathrm{av}}$ mixing is reduced and at a sufficiently high Z and charge state the oscillator strength becomes concentrated in the $4d^{10} \rightarrow 4d^9 4f^1P_1$ transition. Consequently, in Xe-like ions, one very strong line should eventually dominate the subthreshold spectrum [21,29]. Indeed, in progressing from Xe^{5+} to Xe^{7+} it was found that the spectrum in each case contained only a few strong lines which could be labeled as (with one for each n) $4d^{10}5s^m 5p^k \rightarrow 4d^9 nf 5s^m 5p^k$ transitions. Moreover, the calculated intensity of the feature resulting from $4d^{10} \rightarrow 4d^9 4f$ transitions increased in intensity, while both the observed and predicted ratio of the $4d^{10} \rightarrow 4d^9 5f$ to the $4d^{10} \rightarrow 4d^9 4f$ features decreased with increasing ionization. The degree of $4f$ collapse therefore determines the intensity distribution among the observed $4d \rightarrow nf$ transitions.

The degree of collapse has also been demonstrated to influence the width of the $4d^{10} \rightarrow 4d^9 4f^1P_1$ feature in Xe-like La^{3+}, whose nonradiative decay rate is determined by the electrostatic $R^k(4f5p,4d\varepsilon l)$ integral and so by the degree of $4d,4f$ overlap [30]. In Sb^+ through Sb^{3+}, I^{2+}, Xe^+, Xe^{2+}, Cs^+ and Ba^{2+}, the $4d \rightarrow 4f$ lines are relatively narrow, indicating that the $4f$ is only partially collapsed. In La^{3+}, by contrast, the spectrum consists of a broad, intense $4d^{10} \rightarrow 4d^9 4f^1P_1$ transition with a width of $\sim$2 eV and a series of weaker $4d \rightarrow nf$ $(n>4)$ transitions [10]. In Ce^{4+}, the predicted width of the $4d \rightarrow 4f^1P$ feature is 1.77 eV [31] and again it is expected to dominate the spectrum. However, with the exception of Xe^{3+} and La^{3+}, no other direct observation of $4f$ collapse and the attendant transfer of oscillator strength from a broad continuum resonance to broad subthreshold features has been reported. Here it is shown that the behavior in the Cs isonuclear sequence is very similar to that observed along the Xe isoelectronic sequence.

II. EXPERIMENT

In the earlier experiment on Cs^+ [3], which was performed using photographic detection, absorption saturation made it impossible to extract any meaningful information on relative line intensities or to infer the profile of the continuum resonance. In the present work, spectra were recorded photoelectrically with a 1024-element silicon photodiode array using the DLP method [32]. The detector array was fiber-optically coupled to an image-intensified microchannel plate assembly, mounted on a 2-m grazing incidence vacuum spectrograph to give a photon energy resolution, $E/\Delta E$, of $\sim 1.5 \times 10^3$. Because of the difficulty of handling pure cesium targets, a 1-J, 25-ns ruby laser pulse was focused to a 200-μm-diameter focal spot on compressed pellets of CsCl and CsBr to form the absorbing plasma, while the backlighting continuum was provided by radiation from a tungsten plasma produced by an 860-mJ, 10-ns Q-switched Nd:YAG laser pulse. The halogen atoms and ions have rather smooth photoabsorption cross sections and yield no rapidly varying structure in the region of interest. By altering the interlaser time delay, the on-target laser irradiance, or probing different plasma regions, absorption from a particular ion stage could be optimized. Five spectra, obtained at time delays of 25, 40, 140, 450, and 1,500 ns, are presented in Fig. 1. At the maximum time delay, the spectrum is primarily that of neutral cesium, while at the intermediate delays it contains both Cs^+ and Cs^{2+} absorption. At the shortest delay, the spectrum is dominated by Cs^{3+} and Cs^{4+} absorption; however, the latter proved impossible to isolate in the series of experiments reported here. Verification of the identity of the absorbing species was provided by the subsequent observation of the absorption of the $4d^{10}5s^2 5p^k - 4d^9 5s^2 5p^{k+1}$ multiplet in the relevant charge state under similar experimental conditions.

III. RESULTS AND DISCUSSION

The spectra of Cs, Cs^+, and Cs^{2+} are dominated by a $4d \rightarrow \varepsilon f$ continuum resonance and clearly show the intensity enhancement of discrete structure with increasing ionization. Since such phenomena are essentially many-body in nature involving collective excitation of the $4d$ subshell electrons,

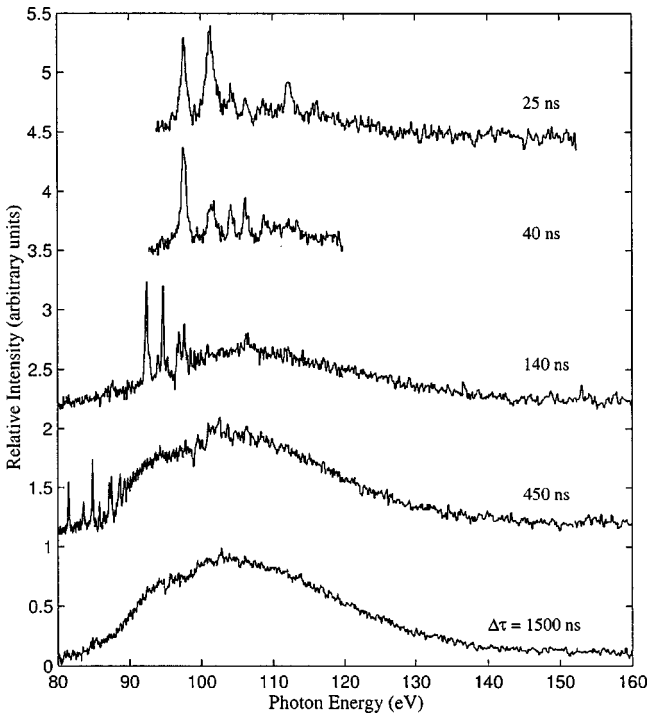

FIG. 1. Photoabsorption spectra from laser-produced plasmas of cesium recorded with the dual laser-produced plasma technique at time delays ranging from 25 ns to 1500 ns after their generation. The cesium plasmas were produced by a 1000-mJ, 25-ns ruby laser pulse, focused to a 200-μm diameter spot on a CsCl pellet. The backlighting XUV continuum was provided by focusing an 860-mJ, 10-ns, Nd:YAG pulse onto a tungsten target.

the appropriate theoretical description should reflect this. A number of theoretical prescriptions exist such as many-body perturbation theory [33], the random phase approximation with exchange (RPAE) [34,35] and the local-density-based random phase approximation [24,36]. Calculations for Cs have previously been performed using the RPAE method both with and without inclusion of outer shell correlations [37]. For Cs^+, relativistic random phase approximation (RRPA) calculations where six interacting continuum channels were included, namely, $4d_{3/2} \rightarrow p_{1/2}, p_{3/2}, f_{5/2}$ and $4d_{5/2} \rightarrow p_{3/2}, f_{5/2}, f_{7/2}$, predicted a peak cross section of 36 Mb near 105 eV [29]. Yet another theoretical approach is provided by the time-dependent local density approximation [38]. This method has recently been shown to be very useful for studying changes in the $4d$ cross section with increasing ionization in iodine [15]. In the work reported here, the relativistic time-dependent local density approximation (RTDLDA) code DAVID [39] was used to calculate the continuum cross section of each species above the $4d$ threshold. In neutral Cs, it predicts a peak cross section of 30 Mb at an energy of ~107 eV, in Cs^+ it predicts a peak cross section of 30 Mb at an energy of ~107 eV, while in Cs^{2+} it again yields a value of 30 Mb at 106 eV. The RTDLDA-calculated cross sections are shown in Figs. 2–4 along with the corresponding experimental spectra. It should be noted that the absolute cross section has not been determined experimentally here, and hence the experimental spectra are simply scaled linearly in order to match them to the calculated ones.

In the original experiment, which yielded the neutral spectrum, the shape of the $4d \rightarrow \varepsilon f$ resonance could only be inferred because of absorption saturation of the peak [1]. In Fig. 2, the present experimental spectrum is compared with the RTDLDA result and also RPAE calculations with and without outer shell correlations [37]. The former appears to give optimum agreement, while the discrepancy at the leading edge is due to the presence of double electron transitions. This is particularly interesting since correlation effects arising from outer $5s$ and $5p$ electrons, which tend to broaden and depress the peak height, were not included. Also included in this figure are the results of a single particle calculation for $4d \rightarrow \varepsilon f$ photoexcitation performed with wave functions calculated using the Cowan suite of codes [40]. The continuum cross sections were calculated using [41]

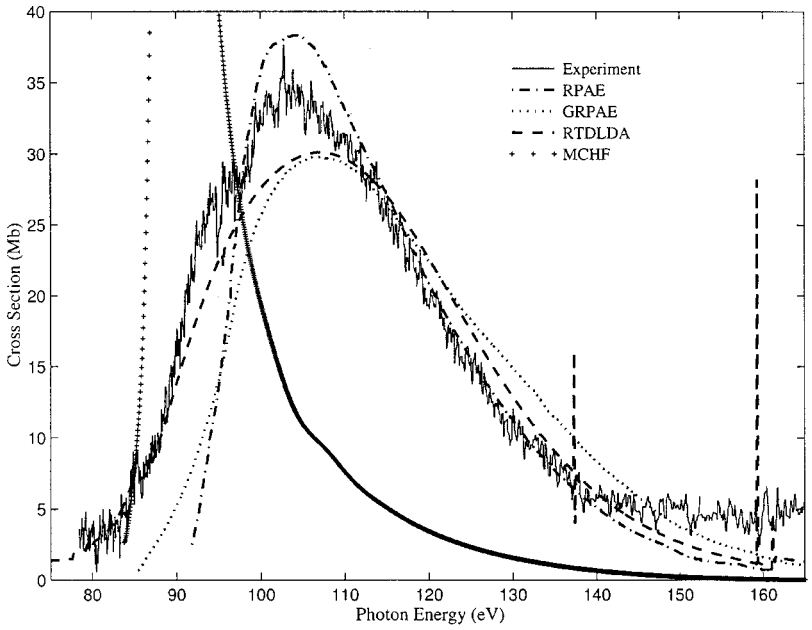

FIG. 2. Photoabsorption spectrum of neutral Cs compared with the results of many-body calculations performed within the random phase approximation with exchange, with GRPAE and without RPAE correlation [32], RTDLDA, and single-particle Hartree-Fock calculations with the Cowan code [35]. Since it was only possible to measure the relative absorption cross section, the results are fitted to the theoretically determined cross-section data.

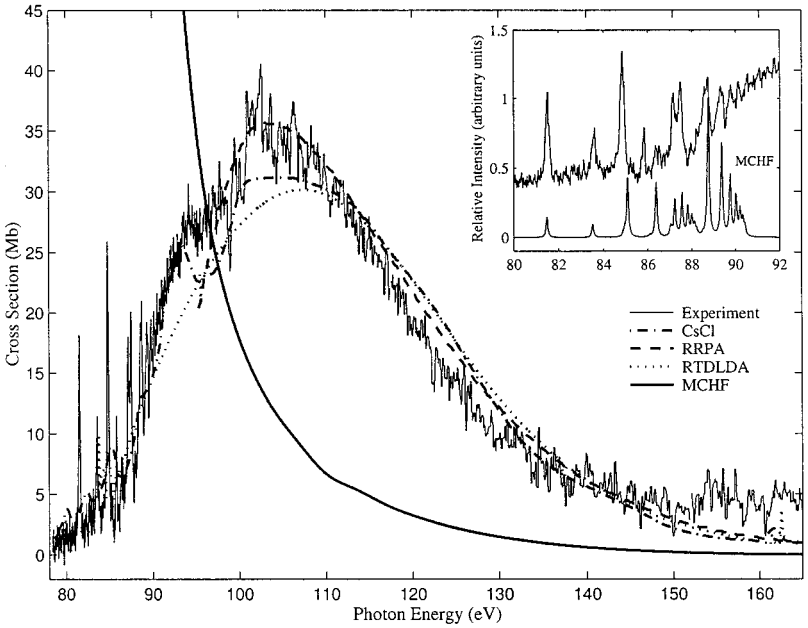

FIG. 3. Photoabsorption spectrum of Cs^+. The continuum absorption is compared with the experimental absorption spectrum of CsCl [38] and the results of RRPA [26], RTDLDA, and single-particle Hartree-Fock calculations with the Cowan code [35]. Since it was only possible to measure the relative absorption cross section, the results are fitted to the theoretically determined cross-section data. The discrete spectral features (insert) are compared with the results of MCHF calculations.

$$\sigma(4d\rightarrow\varepsilon f)=8\pi\alpha a_0^2(\varepsilon-\varepsilon_{4d})|\langle 4d|r|\varepsilon f\rangle|^2$$

where $\varepsilon-\varepsilon_{4d}$ is the energy required to produce an electron with kinetic energy ε following direct $4d$ ionization. This calculation, in which a single discrete $4f$ state was included in the excited state basis to allow for $4f$, εf interaction, predicts the continuum cross section to peak near 90 eV. This value is ~12 eV too low in energy and yields a maximum cross section of 145 Mb that is four to five times too large. However, these results are consistent with other predictions based on single-particle models [15,41] and highlight the necessity of including many-body effects. Between 80 and 90 eV, the experimental spectrum contains a number of weak discrete features which were found to arise from $4d\rightarrow 6p$, $7p$ and $8p$ transitions converging on the $4d^9 6s(5/2,1/2)j$ and $(3/2,1/2)j$ limits of Cs^+ [1]. Considerable information on the $4d\rightarrow\varepsilon f$ behavior of Cs^+ is already indirectly available from comparisons between the spectra of atomic cesium and cesium halides [42,43] and from electron impact ionization studies [44–46]. In solid CsCl, where the absorption is essentially due to Cs^+, albeit in a solid environment, the $4d\rightarrow\varepsilon f$ peak was found to be shifted to lower energy compared to the neutral case and to contain more structure. In particular, double electron excitations of the type $4d^{-1}5p^{-1}$ are responsible for a steep rise near 90 eV and well-developed features between 90 and 100 eV. Extensive calculations have been performed for double electron excitations of the type $4d^{10}5s^25p^6\rightarrow 4d^95s^25p^5nln^1l^1$, $4d^{10}5s^25p^6\rightarrow 4d^95s5p^6nln^1l^1$, and $4d^{10}5s^25p^6\rightarrow 4d^85s^25p^6nln^1l^1$ with the RCN, RCN2, and RCG suite of programs developed by Cowan [40]. These calculations predict the onset of $4d^{-1}5p^{-1}$ excitation to occur near 95 eV and not 90 eV as observed; $4d^{-1}5s^{-1}$ excitation is calculated to begin at 116 eV and double $4d$ excitation to commence at 165 eV. Many of these transitions are predicted to have oscillator strengths in the 10^{-6} range, and the oscillator strength envelope has a pronounced minimum at 114 eV. In Fig. 3, direct comparison is made between the RRPA, RTDLDA, halide results, and the ion spectrum. In particular, the RRPA results, which ignore correlations with the $5s$ and $5p$ subshells, seem to agree very well with the experimental profile obtained. Once more a single-particle calculation was performed. As in the neutral case, it again yields a maximum cross section of 145 Mb just at threshold that points to the fact that the wave functions used, which were derived in an average energy of configuration calculation and thus are not εf^1P_1 functions, overestimate the degree of core penetration in this ion. The discrete structure present in the Cs^+ spectrum, was previously identified [3] and the results of these calculations, performed with a 50% scaling of Slater-Condon parameters, are included in this figure. Note, that unlike the neutral case, transitions to discrete nf orbitals are observed, although the narrowness of the resulting linewidths indicates that the degree of orbital collapse is minimal. However, the calculations [3] were found to overestimate the relative strength of the $4d\rightarrow nf$ transitions and, by extension, their $4f_{\mathrm{av}}$ composition and/or the degree of *f*-collapse.

For Cs^{2+}, the energy level positions, oscillator strengths, and linewidths of the discrete features were determined in a configuration interaction calculation using a basis that consisted of $4d^9nf$ and $4d^9np$ Hartree-Fock (E_{av}) functions ($4\leqslant n\leqslant 10, 6\leqslant n\leqslant 9$) and a discretized continuum with the Cowan suite of codes. In constructing the computed cross sections, the discrete features were assumed to have a Lorentzian profile and the resonant parts of the cross sections were calculated using the formula $\sigma(\mathrm{Mb})=109.7\Gamma_k f_k\{2\pi(E_k-E)^2+\Gamma_k^2/4\}^{-1}$ where E_k and Γ_k are the energy and linewidth of the transition (in eV) and f_k is the oscillator strength. The autoionization widths were calculated directly by allowing for the decay processes $4d^95s^25p^5nl\rightarrow 4d^{10}5s^25p^3nl+\varepsilon l$, $4d^{10}5s^25p^4+\varepsilon l$, $4d^{10}5p^5nl+\varepsilon l$, $4d^{10}5s5p^4nl+\varepsilon l$, and $4d^{10}5s5p^5+\varepsilon l$. In Cs^{2+}, an average autoionization width of 50 meV was ob-

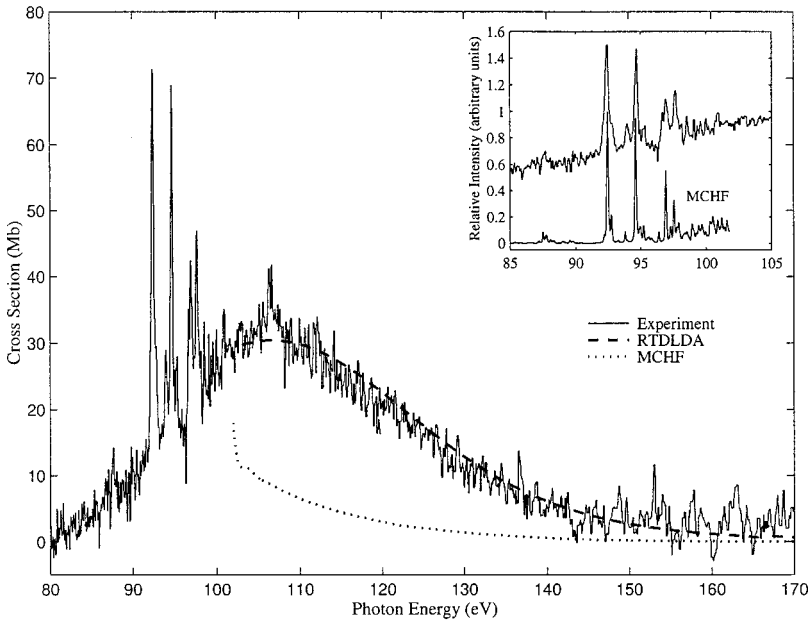

FIG. 4. Photoabsorption spectrum of Cs^{2+}. The continuum absorption is compared with the results of RTDLDA and single-particle Hartree-Fock calculations with the Cowan code [35]. Since it was only possible to measure the relative absorption cross section, the results are fitted to the theoretically determined cross-section data. The discrete spectral features (insert) are compared with the results of MCHF calculations (see text).

tained for the strongest lines (i.e., those with $gf>0.01$), while the average, taking all lines into account, was closer to 20 meV. The results of these calculations are compared with experiment in Fig. 4. Note that in preparing this figure, the above calculations for the discrete part of the spectrum were first shifted uniformly by 0.27 eV towards higher energy to gain optimum agreement with experiment. From Fig. 4, it would appear that the peak cross section of the discrete transitions is close to 70 Mb. In Xe^{4+}–Xe^{7+}, the calculated peak heights of similar features varied from 200 to 900 Mb. It must also be remembered that these features are composites of many overlapping transitions and small differences in position can lead to large differences in both peak height and width. Here, to get the calculated cross section for the discrete features to blend smoothly with the RTDLDA results for the continuum part and be in qualitative agreement with the observed spectrum, it was necessary to divide the theoretical result by a factor close to 10. The difference between theory and experiment is primarily due to absorption saturation of the peaks (which is particularly evident in higher stages) along with plasma broadening effects that combine to reduce the peak height to linewidth ratios as well as their multicomponent nature. Moreover, this type of calculation places the maximum of the $4d\rightarrow f$ cross section below threshold, as is evident from the single-particle cross section included in Fig. 4, rather than at $\sim$ 5 eV above it as observed. This result, which suggests that the bulk of the oscillator strength has been transferred to the discrete spectrum, is at variance with observation. Since any overestimate of the degree of wave function collapse will cause an overestimate of linewidth, the fact that the observed linewidth is greater than the calculated one can only be resolved by requiring each feature to be composed of a number of separated individual ''narrow'' lines rather than a closely packed group of ''broad'' lines. For Cs^{2+} through Cs^{4+}, the absorption profiles are further complicated by the fact that the ground configuration of each contains more than one term and in a laser-produced plasma, absorption from all low-lying states that can be thermally populated is obtained. In the Cs^{2+} case, the $^2P_{3/2}-^2P_{1/2}$ interval is well known [47] and the cross sections for absorption from each of these levels were evaluated and summed with a weight appropriate to a particular excitation temperature. This procedure has already been shown to yield good agreement between theory and experiment for $4d\rightarrow 5p$ transitions in ionized Sb and Te [48,49]. Comparison between the calculations and the experimental results for both $4d\rightarrow 5p$ and $4d\rightarrow nf$ spectra indicate that a Boltzmann distribution appropriate to an equilibrium plasma electron temperature of 2 eV gives optimum agreement between theory and experiment.

The detailed assignments of the strongest features will be presented elsewhere. Compared to Cs^{+}, the average oscillator strength of the $4d\rightarrow nf$ transitions in Cs^{2+} is greater but the observed linewidths, along with the presence of a strong $4d\rightarrow \varepsilon f$ feature, again indicates that the $4f$ function is only partially collapsed. The mixing of nf terms, alluded to in the introduction results in an average eigenvector purity only of the order of 20%. The strongest features at 92.44 and 97.70 eV are due to many overlapping transitions to final states, which are predominantly of $5f$ character in the basis used here, although they generally contain admixtures of $4f$, $6p$, and $7p$.

The same procedure was then used to estimate the resonant part of the cross sections in Cs^{3+} and Cs^{4+} (Figs. 5 and 6). In preparing the theoretical plots in these figures, no shifts were employed although it was again necessary to reduce the calculated peak cross sections of the discrete features to get them to scale smoothly into the RTDLDA results. Again, a glance at Figs. 5 and 6 shows that the theoretical widths are less than observed pointing once more to an underestimate of the energy spread of the component lines as well as to plasma broadening and possibly absorption saturation effects as the source of this discrepancy. The energies of the component terms of the ground configura-

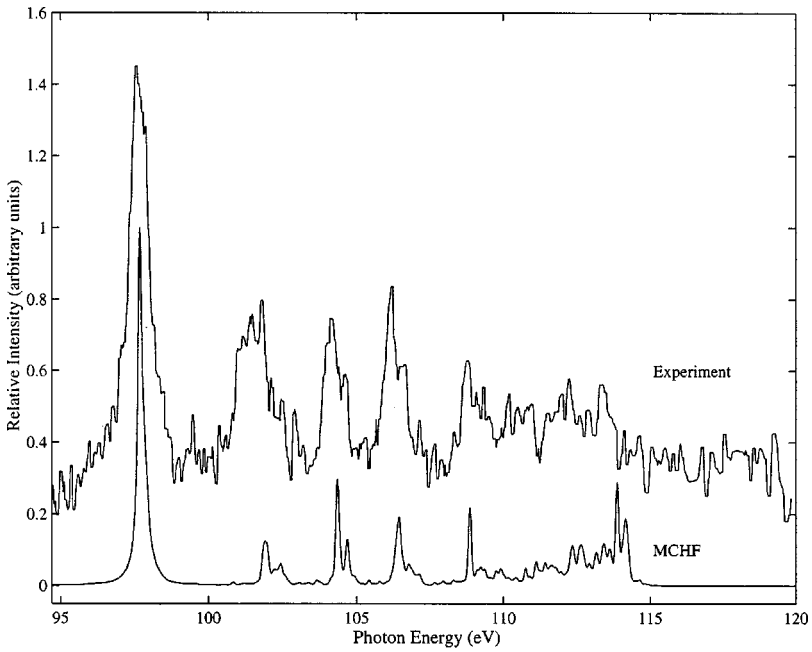

FIG. 5. Photoabsorption spectrum of Cs^{3+} and Cs^{4+} compared with the results of MCHF calculations for Cs^{3+}.

tions are well known in each case [50–52] and these values were used to estimate excited state populations assuming a Boltzmann distribution among the levels as above. A value of $T_e = 2.5\,\mathrm{eV}$ was found to yield optimum agreement with experiment. From Fig. 1 (experiment) and these figures, it is obvious that the $4f$ orbital has contracted abruptly between Cs^{2+} and Cs^{3+}. In Cs^{3+} and Cs^{4+}, average autoionization widths were again calculated directly by allowing for the decay processes $4d^9 5s^2 5p^k 4f \rightarrow 4d^{10} 5s^2 5p^{k-2} 4f + \varepsilon l$, $4d^{10} 5s^2 5p^{k-1} + \varepsilon l$, $4d^{10} 5s 5p^{k-1} 4f + \varepsilon l$, and $4d^{10} 5s 5p^k + \varepsilon l$ and yielded values of 350 and 500 meV, respectively, for the strongest predicted lines. Even allowing for the instrumental linewidth ($\sim$100 meV), these values are smaller than those observed. However, again it must be remembered that each of the observed features are composed of a large number of individual lines. Also, in La^{3+}, this type of calculation underestimated the width of the $4d^{10} 5s^2 5p^6\, {}^1S_0 \rightarrow 4d^9 5s^2 5p^6 4f\, {}^1P_1$ feature by $\sim$50% [10]. So unlike the case of $4d^9 5p^k$ decay where very accurate widths can be obtained [15], problems associated with the best choice of f-wave function make calculation of the widths of $4d^9 5p^k nf$ states less reliable.

The profiles of the configuration average radial wave functions, linear combinations of which can be used to synthesize the eigenfunctions of the observed features and the associated radial potentials, are presented in Fig. 7. They clearly show that the potential barrier vanishes between the first and second ion stages, which is accompanied by a dra-

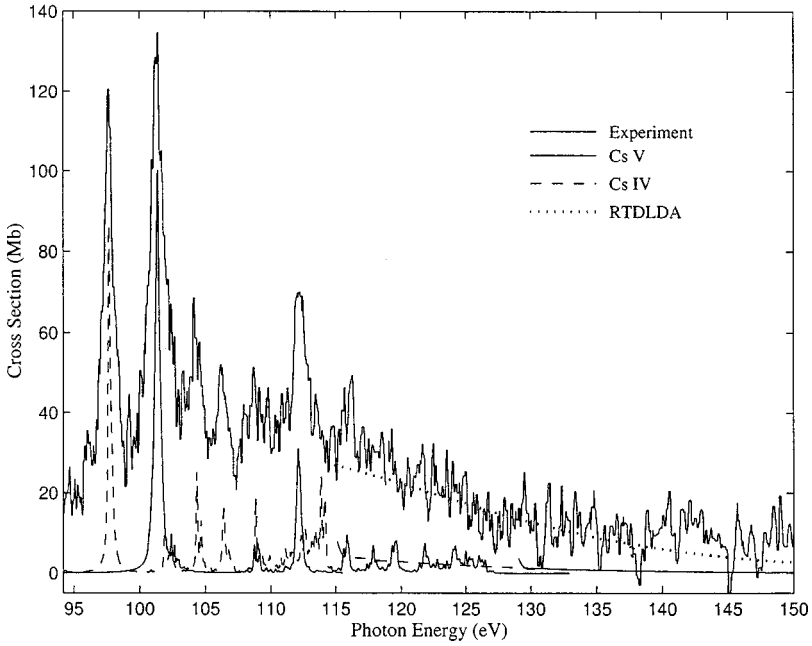

FIG. 6. Photoabsorption spectra of Cs^{3+} and Cs^{4+} compared with the results of multiconfiguration Hartree-Fock calculations for Cs^{4+}. The experimental data are fitted to the results of the RTDLDA calculation for the continuum part of the Cs^{3+} cross section.

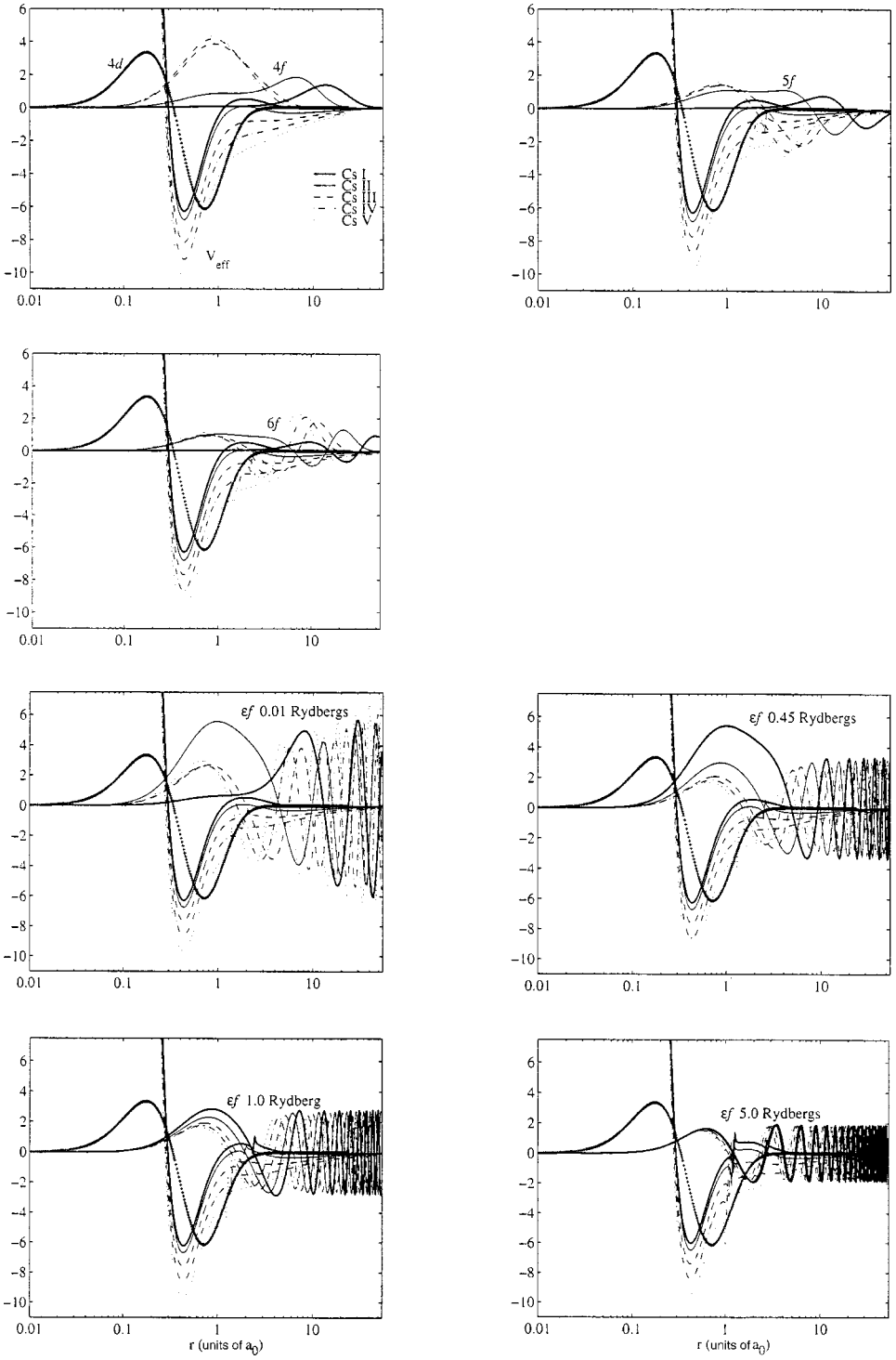

FIG. 7. Variation of radial potential and wave functions for nf_{av} and εf wave functions in cesium with increasing ionization.

matic contraction of the nf functions, particularly the $4f$. As already pointed out, an inspection of the eigenvector composition clearly shows that in Cs^{2+} the strongest lines consist of mixtures of $4f$ and higher nf and np states and are in general more ''$5f_{\mathrm{av}}$'' in character than ''$4f_{\mathrm{av}}$.'' For example, the strongest lines in the spectrum at 92.44 and 94.70 eV are primarily due to $^2P_{3/2}\rightarrow{}^2D_{5/2}$ and $^4F_{5/2}$ transitions. The former is only 13% $4f$, but more than 40% $5f$ in character, while the latter is virtually 100% $5f$. In Cs^{3+}, the situation is quite different and the feature at 97.65 eV is primarily due to a $^3P_2\rightarrow 4f^3D_3$ transition, with the eigenvector being composed of admixtures of different $4f$ states. In general, the degree of nf mixing decreases with increasing ionization. Indeed, in Cs^{3+} the strongest features at 97.65, 104.15, and 106.20 eV can be assigned as essentially $4d\rightarrow 4f$, $4d\rightarrow 5f$, and $4d\rightarrow 6f$ transitions. In Cs^{4+}, the strong features at 101.38 and 112.20 eV can again be assigned unambiguously as $4d\rightarrow 4f$ and $4d\rightarrow 5f$, each composed of thousands of individual overlapping transitions.

Thus, once nf mixing has been included, these calcula-

tions are successful in explaining the dramatic shift of oscillator strength from the continuum to the discrete spectrum that occurs between Cs^{2+} and Cs^{3+}. They also show that the strongest transitions, regardless of the parent or final term, always occur at essentially the same energy that is consistent with earlier predictions [24,25]. Thus, although thousands of individual lines are involved, the spectra are relatively simple and only a tiny fraction of available transitions have any appreciable oscillator strength. A similar phenomenon has been observed in $4d^n \rightarrow 4d^{n-1}4f$ transitions in highly ionized species [53,54] and indeed is a general feature of ionic photoabsorption [55]. There, it has its origin in the strength of the $4d$, $4f$ electrostatic interaction (and therefore, degree of collapse) that causes transitions based on strongly LS coupled $4d^{10}\,{}^1S_0 \rightarrow 4d^9 4f\,{}^1P_1$ parents to dominate. For these species, the $5p$, $5p$ interaction is unchanged since the $5s^2 5p^k$ is essentially ''frozen'' and the $5p$, $4d$, and $5p$, $4f$ interactions are small by comparison. Also, as a result of the weakness of $4d^{10}\,{}^1S_0 \rightarrow 4d^9 4f\,{}^3P_1$ and ${}^3D_1$ components, transitions to only a small subset of lower multiplicity final states dominate the spectra. In the present case, the strong $4d$-$4f$ electrostatic interaction again causes transitions based on strongly LS-coupled $4d^{10}\,{}^1S_0 \rightarrow 4d^9 4f\,{}^1P_1$ parents to dominate. Moreover, since the autoionization linewidths are comparable to the array widths, the strongest transitions will arise from $4d^{10}\,{}^1S_0 \rightarrow 4d^9 nf\,{}^1P_1$ transitions, with the intensities of the individual features being determined by the degree of $4d,nf$ overlap. A similar explanation can be advanced to explain the simplicity of the observed photoionization spectra of ionized Xe. We can thus infer that once oscillator strength has been transferred from the continuum, in any system containing $5s$ or $5p$ electrons, the spectrum will consist of a Rydberg-like series of $4d^{10}\,{}^1S_0 \rightarrow 4d^9 nf\,{}^1P_1$ transitions with the oscillator strength of the first member increasing relative to the others as the degree of ionization is increased.

IV. CONCLUSION

Extreme-ultraviolet (xuv) photoabsorption spectra along the Cs isonuclear sequence from Cs to Cs^{4+} have been observed for the first time. The spectra display clearly the evolution from excitation out of the $4d$-subshell (mainly) into the f continuum to $4d \rightarrow nf$ discrete excitations following f-wave collapse between Cs^{2+} and Cs^{3+}. The results add to the growing body of knowledge on the sensitivity of f-wave functions to the ionization stage for atoms that immediately precede or follow Xe where the degree of localization of f electrons is most likely to be in doubt. Despite the complexity of the physics involved, which includes the need for theoretical prescriptions that can handle either term-dependent or strongly correlated orbitals at the beginning of the sequence to encompass many-configuration interactions for more highly charged ions, current atomic structure and photoionization codes provide quite good agreement with experiment.

ACKNOWLEDGMENTS

This work was supported by the Irish Science and Technology Agency Enterprise Ireland under research Grant No. SC-99-206. The assistance and helpful suggestions of Ronan Faulkner, Padraig Dunne, and Emma Sokell of University College Dublin, at different stages of this work, is gratefully acknowledged.

[1] H. Petersen, K. Radler, B. Sonntag, and R. Haensel, J. Phys. B **8**, 31 (1975).
[2] T. J. McIlrath, J. Sugar, V. Kaufman, D. Cooper, and W. T. Hill, J. Opt. Soc. Am. B **3**, 1986 (1986).
[3] A. Cummings and G. O'Sullivan, J. Phys. B **30**, 5599 (1997).
[4] J. M. Bizau, J.-M. Esteva, D. Cubaynes, F. J. Wuilleumier, C. Blancard, A. Compant La Fontaine, C. Couillaud, J. Lachkar, R. Marmoret, C. Remond, J. Bruneau, D. Hitz, P. Ludwig, and M. Delaunay, Phys. Rev. Lett. **84**, 435 (2000).
[5] H. Kjeldsen, J. B. West, F. Folkmann, H. Knudsen, and T. Andersen, J. Phys. B **33**, 1403 (2000).
[6] M. Oura, T. M. Kojima, Y. Awaya, Y. Itoh, K. Kawatsura, M. Kimura, T. Koizumi, T. Sekioka, H. Yamaoka, and M. Cox, J. Synchrotron Radiat. **5**, 1058 (1998).
[7] B. Rouvellou, J. M. Bizau, J. Obert, S. Al Moussalami, N. Berland, C. Blancard, E. Bouisset, D. Cubaynes, S. Diehl, L. Journel, J. C. Putaux, C. Vinsot, and F. J. Wuilleumier, Nucl. Instrum. Methods Phys. Res. B **134**, 287 (1998).
[8] A. Gottwald, C. Gerth, and M. Richter, Phys. Rev. Lett. **82**, 2068 (1999).
[9] T. B. Lucatorto, T. J. McIlrath, J. Sugar, and S. M. Younger, Phys. Rev. Lett. **47**, 1124 (1981).
[10] U. Köble, L. Kiernan, J. T. Costello, J. P. Mosnier, E. T. Kennedy, V. K. Ivanov, V. A. Kupchenko, and M. S. Shendrik, Phys. Rev. Lett. **78**, 2188 (1995).
[11] M. Sano, Y. Itoh, T. Koizumi, T. M. Kojioma, S. D. Kravis, M. Oura, T. Sekioka, N. Watanabe, Y. Awaya, and F. Koike, J. Phys. B **29**, 5305 (1996).
[12] N. Watanabe, Y. Awaya, A. Fijino, Y. Itoh, M. Kitajima, T. M. Kojima, M. Oura, R. Okuma, M. Sano, T. Sekioka, and T. Koizumi, J. Phys. B **31**, 4137 (1998).
[13] T. Koizumi, Y. Awaya, A. Fujima, Y. Itoh, M. Katajima, M. Kojima, M. Oura, R. Okima, M. Sano, T. Sekioka, N. Watanabe, and F. Koike, Phys. Scr. **T73**, 131 (1997).
[14] T. Koizumi, Y. Itoh, M. Sano, M. Kimura, T. M. Kojima, S. Kravis, A. Matsumoto, M. Oura, T. Sekioka, and Y. Awaya, J. Phys. B **28**, 609 (1995).
[15] G. O'Sullivan, C. McGuinness, J. T. Costello, E. T. Kennedy, and B. Weinmann, Phys. Rev. A **53**, 3211 (1996).
[16] R. M. D'Arcy, J. T. Costello, E. T. Kennedy, J. P. Mosnier, C. McGuinness, and G. O'Sullivan, J. Phys. B **33**, 1383 (2000).
[17] J. P. Connerade, *Highly Excited Atoms* (Cambridge University Press, Cambridge, 1998).
[18] R. I. Karaziya, Sov. Phys. Usp. **24**, 775 (1981).
[19] K. Nuroh, M. J. Stott, and E. Zaremba, Phys. Rev. Lett. **49**, 862 (1982).

[20] G. O'Sullivan, J. Phys. B **15**, L765 (1982).
[21] K. T. Cheng and C. Froese Fischer, Phys. Rev. A **28**, 2811 (1983).
[22] S. Kucas, A. Kariosiene, and R. Karaziya, Liet. Fiz. Rinkinys **23**, 34 (1983) [Lith. Phys. J. **28**, 36 (1983)].
[23] C. W. Clarke and T. B. Lucatorto, in *Giant Resonances in Atoms, Molecules and Solids*, edited by J. P. Connerade, J. M. Esteva, and R. C. Karnatak [Plenum, New York, 1987].
[24] G. Wendin, in *Giant Resonances in Atoms, Molecules and Solids*, Vol. 151 of *NATO ASI Series B: Physics*, edited by J. P. Connerade, J. M. Esteva, and R. C. Karnatak (Plenum Press, New York, 1987), p. 179.
[25] Z. Crljen and G. Wendin, Phys. Rev. A **35**, 1571 (1987).
[26] J. P. Connerade and M. W. D. Mansfield, Phys. Rev. Lett. **48**, 131 (1982).
[27] J. E. Hansen, A. W. Flifet, and H. P. Kelly, J. Phys. B **8**, L127 (1975).
[28] G. Wendin and A. F. Starace, J. Phys. B **11**, 4119 (1979).
[29] K. T. Cheng and W. R. Johnson, Phys. Rev. A **28**, 2820 (1983).
[30] J. E. Hansen, J. Brilly, E. T. Kennedy, and G. O'Sullivan, Phys. Rev. Lett. **63**, 1934 (1989).
[31] V. K. Ivanov, in *Proceedings of the Tenth VUV Conference*, Paris, 1992, edited by F. J. Wuilleumier, Y. Petroff, and I. Nenner (World Scientific, Singapore, 1993), p. 178.
[32] E. T. Kennedy, J. T. Costello, J. P. Mosnier, A. A. Cafolla, M. Collins, L. Kiernan, U. Koble, M. H. Sayaad, M. Shaw, B. F. Sonntag, and R. Barchewitz, Opt. Eng. (Bellingham) **33**, 3926 (1995).
[33] H. P. Kelly, Phys. Scr. **T17**, 109 (1987).
[34] M. Ya. Amusia, V. K. Ivanov, and L. V. Chernisheva, Phys. Lett. **50A**, 194 (1976).
[35] G. Wendin, in *X-Ray and Inner Shell Physics*, edited by B. Crasemann, No. 94 (AIP, Woodbury, New York, 1982), p. 495.
[36] G. Wendin, in *New Trends in Atomic Physics*, edited by G. Grynberg and R. Stora (Elsevier, New York, 1984), p. 555.
[37] M. Ya. Amusia, *Atomic Photoeffect* (Plenum, New York, 1990).
[38] A. Zangwill and P. Soven, Phys. Rev. A **21**, 1561 (1980).
[39] D. A. Liberman and A. Zangwill, Comput. Phys. Commun. **32**, 75 (1984).
[40] R. D. Cowan, *The Theory of Atomic Structure and Spectra* (University of California Press, Berkeley, 1981).
[41] S. T. Manson and J. W. Cooper, Phys. Rev. **165**, 126 (1968).
[42] M. Cardona, R. Haensel, D. W. Lynch, and B. Sonntag, Phys. Rev. B **2**, 1117 (1970).
[43] K. Radler and B. Sonntag, Chem. Phys. Lett. **39**, 371 (1976).
[44] D. R. Hertling, R. K. Feeney, D. W. Hughes, and W. E. Sayle, J. Appl. Phys. **53**, 5427 (1982).
[45] A. Muller, K. Tinschert, G. Hoffman, E. Salzborn, and G. H. Dunn, Phys. Rev. Lett. **61**, 70 (1988).
[46] J. W. G. Thomason, B. Peart, and S. J. T. Hayton, J. Phys. B **30**, 749 (1996).
[47] G. Epstein and J. Reader, J. Opt. Soc. Am. **66**, 590 (1976).
[48] R. M. D'Arcy, J. T. Costello, C. McGuinness, and G. O'Sullivan, J. Phys. B **32**, 4859 (1999).
[49] N. Murphy, J. T. Costello, E. T. Kennedy, C. McGuinness, J. P. Mosnier, B. Weinmann, and G. O'Sullivan, J. Phys. B **32**, 3905 (1999).
[50] J. Reader, J. Opt. Soc. Am. **73**, 349 (1983).
[51] A. Tauheed and Y. N. Joshi, J. Phys. B **27**, 405 (1994).
[52] A. Tauheed and Y. N. Joshi, Phys. Scr. **47**, 550 (1993).
[53] G. O'Sullivan and P. K. Carroll, J. Opt. Soc. Am. **71**, 227 (1981).
[54] J. Bauche, C. Bauche-Arnoult, and M. Klapisch, Phys. Rev. A **28**, 829 (1983).
[55] J. Tullki and T. Aberg, J. Phys. B **22**, 3681 (1989).